

Entropy and boundary conditions in random rhombus tilings

This article has been downloaded from IOPscience. Please scroll down to see the full text article.

1998 J. Phys. A: Math. Gen. 31 6123

(<http://iopscience.iop.org/0305-4470/31/29/005>)

View [the table of contents for this issue](#), or go to the [journal homepage](#) for more

Download details:

IP Address: 171.66.16.122

The article was downloaded on 02/06/2010 at 06:58

Please note that [terms and conditions apply](#).

Entropy and boundary conditions in random rhombus tilings

N Destainville

Groupe de Physique des Solides, Tour 23-24, 5^e étage, Universités Paris 7 et 6, 2, place Jussieu, 75251 Paris Cedex 05, France

Received 31 March 1998

Abstract. The tilings of rhombi in two dimensions and of rhomboedra in three dimensions are studied when they are constrained by fixed boundary conditions. We establish a link between those conditions and free or periodic boundary ones: the entropy is written as a functional integral which is treated via a saddle-point method. We can exhibit the dominant states of the statistical ensemble of tilings and show that they can display a strong structural inhomogeneity caused by the boundary. This inhomogeneity is responsible for a difference of entropy between the studied fixed boundary tilings and free boundary ones. This method uses a representation of tilings by membranes embedded in a higher-dimensional hypercubic lattice. It is illustrated in the case of 60 degree rhombus tilings.

Introduction

Since the discovery of quasicrystals in 1984 [1], a great deal of work has been accomplished to get a precise microscopic structural description of these metallic non-crystalline alloys. It was rapidly understood that Penrose-like [2] tilings could provide very good microscopic models of quasicrystals: it is highly presumed that favoured atomic motifs form tiles. However, the best description for real quasicrystals remains an open question: according to the mechanisms involved to describe the structure and explain its stability, the studied tilings can be perfect Penrose-like arrangements of tiles or random ones. Indeed, despite their random character, the latter exhibit global quasiperiodic symmetries [3,4] and are therefore good candidates for quasicrystal models. The random tilings use the same tiles as the perfect ones. However, in the former, local rearrangements of tiles—called localized phason flips—are allowed. These degrees of freedom give access to a great number of microscopic configurations. This is the random tiling model (RTM) [5, 6, 4]. It involves an important contribution of the tiling entropy to the total configurational entropy, and therefore to the free energy. This phenomenon is supposed to favour the quasicrystal against other competitive phases.

Among the different techniques developed to estimate this tiling configurational entropy, the partition method [7–11] presents the advantage to set a particularly well-defined combinatorial problem. However, the boundary conditions of the tilings considered in this method are different from the usual ones. As a consequence, the configurational entropy per tile of partition tilings is lower than the usual free boundary one: in the simplest case of 60 degree rhombus tilings, the respective values can be exactly calculated and are about 0.261 [7] and 0.323 [12] at the infinite-size limit when the three fractions of tiles are equal

(the configurational entropy per tile is simply the logarithm of the number of tilings divided by the number of tiles).

Elser [7] offered a qualitative argument to explain this difference. The goal of this paper is to go further: we shall establish the link between the different kinds of boundary conditions and we shall give a qualitative as well as quantitative explanation for the difference of entropy per tile. Hence, we shall connect two related models of statistical mechanics, which are usually treated via rather unrelated methods.

A preliminary part of these results was briefly exposed in [10]. Most of them were concisely presented in a shortened version during the Sixth International Conference on Quasicrystals (ICQ6), in Tokyo [13].

1. Random rhombus tilings and boundary conditions

In this paper, we shall consider d -dimensional tilings of rhombic tiles (rhombi in two dimensions, rhomboedra in three dimensions) which tile a region of the Euclidean space, without gaps or overlaps. The standard method for generating such structures consists of a selection of sites and tiles in a D -dimensional lattice ($D > d$) according to certain rules, followed by a projection onto a suitable d -dimensional subspace and along a generic direction. We then say that we have a $D \rightarrow d$ tiling problem. It is the so-called ‘cut-and-project’ method [3, 14, 15]. By construction, the so-obtained rhombic tiles are the projections of the d -dimensional facets of the D -dimensional hypercubic lattice. There are $\binom{D}{d}$ different species of tiles. In the simple $3 \rightarrow 2$ case, this amounts to three kinds of differently oriented 60 degree rhombi.

Usually, those tilings have periodic or free boundary conditions and it is generally admitted that the respective entropies are equal at the thermodynamic limit—for given fractions of tiles. In the following, we shall consider fixed boundary conditions [10], related to the partition method. The region to be tiled will be the generic ‘shadow’ of a D -dimensional rectangular parallelepiped, the sides of which take integer lengths in the D -dimensional hypercubic lattice. This generic shadow is called a zonotope [16], denoted by \mathcal{Z} . When $d = 2$, the zonotopes coincide with the $2D$ -gons. The tiles are supposed to perfectly fit with the boundary $\partial\mathcal{Z}$ of \mathcal{Z} . Examples of $3 \rightarrow 2$ tilings are given in figures 1 and 3.

The entropy per tile is a function of the different fractions of tiles, or in other words a function of the side lengths of the zonotope \mathcal{Z} . For example, the $3 \rightarrow 2$ tilings are enumerated by MacMahon’s formula [17], which was derived at the beginning of this century:

$$W_{k,l,p}^{3 \rightarrow 2} = \frac{(k+l+p-1)!^{[2]}(k-1)!^{[2]}(l-1)!^{[2]}(p-1)!^{[2]}}{(k+p-1)!^{[2]}(l+p-1)!^{[2]}(k+l-1)!^{[2]}}. \quad (1)$$

Here, this formula has been rewritten in terms of second-order generalized factorial functions [8]:

$$k!^{[0]} = k \quad k!^{[m]} = \prod_{j=1}^k j!^{[m-1]}. \quad (2)$$

The quantities k , l and p denote the side lengths of the hexagonal boundary. The case when all these lengths are equal will be called *diagonal* in the following, and the corresponding entropies will be called diagonal entropies.

In appendix A.2, we rederive this formula via a purely combinatorial method which will prove to be useful in the following, the Gessel–Viennot method [18, 19].

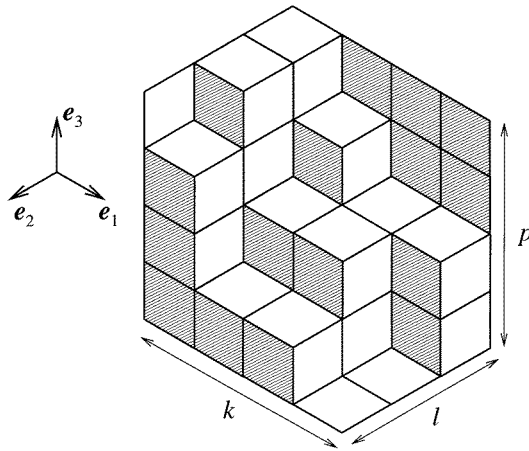


Figure 1. Three-dimensional representation of a $3 \rightarrow 2$ tiling.

In the following we shall be interested in the infinite-size limit entropy of such tilings when the different fractions of tiles are given. This amounts to making the side lengths of the boundary tend to infinity with their relative ratios held fixed: the number of tiles goes to infinity while the shape (but not the size) of the boundary is kept fixed.

2. Continuous limit and functional integral

2.1. Membrane representation of tilings

This point was already developed in previous publications [4, 10, 11] and is closely related to the cut-and-project method. Therefore we shall only give a brief presentation of this method. The main idea is that a random tiling can be lifted as a d -dimensional non-flat structure embedded in a D -dimensional space.

This structure is a *continuous membrane* of d -dimensional facets of the \mathbf{Z}^D hypercubic lattice. When this membrane is projected along a suitable direction, the projections of these facets are precisely the tiles that the tilings are made of (section 1); its continuous character guarantees the absence of gaps in the so-obtained tiling. Such a membrane is said to be *directed* to emphasize the fact that its projection does not create any overlap.

For example, figure 1 displays a $3 \rightarrow 2$ tiling, which can also be seen as a two-dimensional non-flat directed membrane embedded in a cubic lattice. To get a tiling, this membrane must be projected along the $(1, 1, 1)$ direction of the cubic lattice. This point of view can be generalized to arbitrary dimensions. This correspondence is always one-to-one.

In this D -dimensional point of view, the d -dimensional space on which the membranes are mapped to get the tilings is called the real space ε . Its perpendicular space is denoted by ε^\perp . For the sake of convenience, we choose the space coordinates to be the d coordinates on ε and the $D - d$ ones on ε^\perp . Since the membranes are directed, they can be seen as mono-valuate functions ϕ from \mathbf{R}^d to \mathbf{R}^{D-d} . More precisely, in the case of fixed boundary conditions, these functions are defined on the zonotopal region \mathcal{Z} of ε .

In the case of free boundary conditions, if the function ϕ has a large-scale global gradient $\nabla\phi = \mathbf{E}$, the random tiling model states that the fractions of tiles are controlled by this gradient and, therefore, the entropy per tile can be written as a function of \mathbf{E} [4]. This gradient is usually called the *phason* gradient.

Boundary conditions in the membrane representation. We now have to define what the fixed boundary conditions of section 1 become in the language of directed membranes. As illustrated in figure 1, we also get a boundary condition in the D -dimensional space: the membrane is inscribed inside a (non-flat) polygon (or polyhedron), the projection of which on the d -dimensional space gives the tiling boundary, $\partial\mathcal{Z}$ [10, 11]. For instance, the boundaries of $3 \rightarrow 2$ tilings are (non-flat) three-dimensional hexagons. We shall call these boundaries the membrane *frames*. Such a frame can be precisely characterized as the inverse image, via the projection, of the boundary of the zonotopal region \mathcal{Z} which is being tiled [11]. It is therefore a subset of the boundary of the hypercube from which \mathcal{Z} originates. This frame results in conditions on the functions ϕ , on the boundary $\partial\mathcal{Z}$ of \mathcal{Z} .

In the case of free or periodic boundary conditions, the functions ϕ have free or suitable periodic conditions on the boundary of the domains \mathcal{D} on which they are defined (here, we use the notation \mathcal{D} instead of \mathcal{Z} to denote domains which might be non-zonotopal).

2.2. Continuous limit

Once a tiling has been ‘lifted’ in the higher-dimensional space, the so-obtained directed membrane has a corrugated aspect, owing to its discrete character. Here, we wish to get rid of this discrete character, at the infinite-size limit, in order to study more regular (‘smoother’) objects, to which analytic tools can be applied. Moreover, these objects will turn out to characterize the macroscopic states of the statistical ensemble of tilings (or membranes). Let us explain how this continuous limit is taken.

So far, we have considered tiles of side length 1. To define the continuous limit, we shall get rid of this discrete character, thanks to a suitable rescaling. For reasons that will become clear in the following, this side length will go to 0 as the number of tiles tends to infinity. The functions which represent the tilings are defined on a domain \mathcal{D} of the real space. If N is the number of tiles in \mathcal{D} , we need to rescale the tilings by a factor $1/N^{1/d}$. Thus in any infinitesimal domain $d^d y$ in \mathcal{D} , the number of tiles goes to infinity when N does. Moreover, we do the same rescaling in the perpendicular space ε^\perp .

Once we have done this rescaling, the tilings are represented by functions ϕ which have quite an irregular aspect at small scales. As it is usually done, for instance in polymer or polymerized membrane theories, we shall treat small-scale fluctuations and large-scale ones in a different way. Large-scale fluctuations are represented by regular functions whereas microscopic ones around the latter functions are integrated in an entropic term. The latter term will have an exponential form, and will therefore be treated via classical methods on functional integrals.

Below, we shall adopt the following terminology: a membrane (or function) which has microscopic fluctuations, or in other words which is the exact representation of a large tiling, will be called *faceted*. A membrane, the fluctuations of which have been integrated in an entropic term, will be called *smooth*. Finally, we shall go on calling a *tile* any d -dimensional facet of a faceted membrane.

Given a smooth membrane ϕ , we can adopt the first naive definition of the entropy of this membrane [10]:

$$s[\phi] = \lim_{N \rightarrow \infty} \frac{\log(\text{Number of } N\text{-tile faceted membranes close to } \phi)}{N}. \quad (3)$$

The important point here is to understand that, thanks to the previous rescaling, ϕ is kept fixed while the number of tiles goes to infinity. This point allows us, among many other things, to work with the same set of functions whatever the system size.

In this definition, we have not characterized what ‘close’ meant. Let us first state that its precise definition is unessential. To understand this point, let us focus on an analogy with a far more simple statistical mechanics problem, where key ideas are easier to catch on to: let us consider a closed box containing a perfect gas. This box is divided into two parts of same volume, A and B , separated by a virtual frontier. Then one wants to know the entropy $\sigma(x_0)$ of the system at the thermodynamic limit under the condition that a fraction x_0 of the molecules are contained in A (and therefore a fraction $1 - x_0$ in B). Of course, this quantity x_0 fluctuates and can only be defined up to a small quantity Δx . We can write

$$\sigma(x_0) = \lim_{N \rightarrow \infty} \frac{\log(\text{Number of configurations such that } x = x_0 \pm \Delta x)}{N} \quad (4)$$

where N is the number of molecules. The important point here is that it can then be proven that this definition of $\sigma(x_0)$ does *not* depend, at the thermodynamic limit, on the precise choice of Δx , provided it is a finite quantity (see [20, p 30], for example, for a discussion on this point).

In particular, if one looks for the more likely value of x_0 , that is for the maximum of $\sigma(x_0)$, one finds $x_0 = 0.5$, still independently of the choice of Δx . In other words, the dominant states are such that x is close, but not exactly equal to x_0 .

This point of view also applies to directed membranes: we shall see in the next paragraph that this is all the more justified since at the infinite-size limit, only a few constraints cause the faceted membranes to be ‘stuck’ to the smooth one, ϕ .

The next step consists of considering a point y_0 and an infinitesimal domain $d^d y$ in \mathcal{D} containing y_0 . This domain is large compared with the tile size, since this size tends to 0. Moreover, since $d^d y$ is infinitesimal, the gradient $\nabla\phi$ can be considered as constant in this domain. Therefore $d^d y$ contains a piece of tiling with an ‘infinite’ number of tiles and a fixed phason gradient $\mathbf{E} = \nabla\phi(y_0)$. This phason gradient is the only constraint on this piece of tiling. In particular, its boundary conditions are free. Hence if $\sigma(\mathbf{E})$ denotes the entropy per tile of a large free boundary tiling of global phason gradient \mathbf{E} , then the number of faceted membranes close to ϕ and defined on $d^d y$ is equal to

$$\mathcal{N}(y_0) = \exp[N(d^d y)\sigma(\nabla\phi(y_0))] \quad (5)$$

where $N(d^d y)$ is the (large) number of tiles of the previous membranes. This number of tiles depends on the domain size (and on the total number of tiles, N):

$$N(d^d y) = N \cdot n(\nabla\phi) d^d y$$

where $n(\nabla\phi)$ is a function, the integral on \mathcal{D} of which is equal to 1. Hence

$$\mathcal{N}(y_0) = \exp[N \cdot n(\nabla\phi(y_0))\sigma(\nabla\phi(y_0)) d^d y]. \quad (6)$$

Hence the total number of membranes close to ϕ on the whole domain \mathcal{D} is given by

$$\mathcal{N}_\phi = \prod_y \mathcal{N}(y) = \prod_y \exp[N \cdot n(\nabla\phi(y))\sigma(\nabla\phi(y)) d^d y]. \quad (7)$$

This product runs on all the infinitesimal domains $d^d y$. Rigorously, since the membranes are to coincide on the boundaries between the different domains, this product should be divided by a boundary correction term. If $N \rightarrow \infty$, the latter infinitesimal domains contain an infinite number of tiles and these boundary terms disappear[†]. The total number of membranes is therefore equal to the product of the individual numbers of membranes in each domain $d^d y$ when N is large.

[†] In other words, the entropy of two infinite-size subsystems in which $\nabla\phi$ is fixed is additive.

In order to simplify the forthcoming calculations, we choose the infinitesimal domains so that they form a hypercubic lattice which divides the large domain \mathcal{D} in small cubes of side a and of volume $a^d = d^d y$. These domains are indexed by Greek letters and their vertices by Latin letters.

We have already seen that if a is small enough, then ϕ can be considered as affine on any domain α . Therefore this function only depends on its values $\phi_{\alpha,i}$ on the vertices i of the domain:

$$\begin{aligned} \mathcal{N}_\phi &= \prod_\alpha \exp[N \cdot n(\mathbf{E}(\phi_{\alpha,i}))\sigma(\mathbf{E}(\phi_{\alpha,i})) d^d y] \\ &= \exp \sum_\alpha [N \cdot n(\mathbf{E}(\phi_{\alpha,i}))\sigma(\mathbf{E}(\phi_{\alpha,i})) d^d y] \end{aligned}$$

which is actually a function $\mathcal{N}(\phi_i)$ of the values ϕ_i on the lattice vertices.

To sum up, we have fixed the global shape of the faceted membranes: they are tied to the lattice vertices. In other words, we have imposed their mean gradient on the domains α to be equal to the gradient of ϕ . It is actually the *only* constraint we have imposed to these membranes which are counted by \mathcal{N}_ϕ . Now, the key point is that this constraint is sufficient to be sure that, at the infinite-size limit, the faceted membranes counted by \mathcal{N}_ϕ tend towards ϕ . Indeed, Henley [4] showed that for any dimension d , if the gradient \mathbf{E} is fixed, if $\Delta h(L)$ denotes the fluctuations in the perpendicular space of directed membranes of linear size L , then

$$\frac{\Delta h(L)}{L} \rightarrow 0 \quad \text{when } L \rightarrow \infty. \quad (8)$$

(More precisely [4], if $d = 1$, then $\Delta h(L) \sim L^{1/2}$, if $d = 2$, then $\Delta h(L) \sim \log L$ and if $d = 3$, then $\Delta h(L)$ is uniformly bounded.)

After the $1/N^{1/d} \sim 1/L$ rescaling, these fluctuations tend to 0 when $N \rightarrow \infty$. Therefore all the membranes counted by \mathcal{N}_ϕ tend uniformly towards ϕ . Hence, they are *close* to ϕ , whatever the precise definition of this term. Finally,

$$s[\phi] = \lim_{N \rightarrow \infty} \frac{\log(\mathcal{N}_\phi)}{N}. \quad (9)$$

Now, the total number of faceted membranes, \mathcal{N} , is given by the integral[†]:

$$\mathcal{N} = \int \prod_i d\phi_i \mathcal{N}(\phi_i) = \int \prod_i d\phi_i \exp \sum_\alpha N [n(\mathbf{E}(\phi_{\alpha,i}))\sigma(\mathbf{E}(\phi_{\alpha,i})) d^d y]. \quad (10)$$

So far, we have discretized the domain \mathcal{D} to be sure that the membranes have infinite number of tiles in any infinitesimal domain α , at the infinite-size limit. Thus \mathcal{N}_ϕ or \mathcal{N} count faceted membranes close to smooth membranes which are *affine* on every such domain. To get rid of this restriction, we shall now take the limit $a \rightarrow 0$. Formally, we write

$$\mathcal{D}\phi = \lim_{a \rightarrow 0} \prod_i d\phi_i$$

and we turn the sum \sum_α into an integral. Thus

$$\mathcal{N} = \int \mathcal{D}\phi \exp \left[N \int_{\mathcal{D}} n(\nabla\phi)\sigma d^d y \right] \quad (11)$$

[†] Rigorously, in the case of free or periodic boundary conditions, the problem is invariant under translations of ϕ_i and this integral \mathcal{N} is divergent. The membrane must be fixed to a point to avoid this divergence. For example, we fix $\phi(y=0) = 0$.

and

$$\mathcal{N}_\phi = \exp \left[N \int_{\mathcal{D}} n(\nabla\phi) \sigma(\nabla\phi) \, d^d y \right]. \quad (12)$$

Therefore

$$s[\phi] = \int_{\mathcal{D}} n(\nabla\phi) \sigma(\nabla\phi) \, d^d y. \quad (13)$$

As foreseen, this expression is independent of the precise characterization of the above ‘closeness’ in the definition of $s[\phi]$.

This way of writing the entropy associated with a smooth membrane ϕ is quite similar to Henley’s [4] (section 6.1). He gets this result thanks to a suitable coarse-graining of the membranes. The coarse-graining of a faceted function is essentially its local mean in a neighbourhood of diameter a_0 of every point \mathcal{D}^\dagger . Nevertheless, in his point of view, a_0 is large but finite, whereas the smooth functions that we consider here integrate the local fluctuations of an *infinite* number of tiles when N becomes infinite. Moreover, there is a technical difference in the two expressions: Henley’s entropy is an entropy per unit area, whereas ours is an entropy per tile. The ratio between these two entropies is actually $n(\nabla\phi)$, the tile density (per unit area).

Indeed, this last quantity directly depends on the phason gradient $\mathbf{E} = \nabla\phi$, since the latter controls the different fractions of tiles and the different tiles do not necessarily have the same area. The entropy per unit area, $n(\nabla\phi)\sigma(\nabla\phi)$, will be denoted by $\tau(\nabla\phi)$.

However, in the codimension-one case, all the tiles have the same area or volume, and equation (13) can be simplified. The tile density, n , does not depend on the phason gradient any longer and can be factorized before the integral. The exact value of n depends on the choice of the rescaling: so far, we have only specified its order of magnitude ($1/N^{1/d}$) but not its exact value. To calculate n , we choose ϕ to be zero everywhere. Therefore $\nabla\phi = 0$ and $\sigma(\nabla\phi) = \sigma_0$. The entropy per tile $s[\phi]$ is also equal to σ_0 , since this membrane has a vanishing gradient. Hence $\sigma_0 = n \int_{\mathcal{D}} \sigma_0 \, d^d y$ and $n = 1/V(\mathcal{D})$, the inverse volume of \mathcal{D} .

In the codimension-one case,

$$s[\phi] = \frac{\int_{\mathcal{D}} \sigma(\nabla\phi) \, d^d y}{V(\mathcal{D})} \quad (14)$$

which is the expression we gave in [10].

To sum up, we have coded the macroscopic states of this statistical ensemble by an internal parameter ϕ , and we have calculated the entropy associated with these states. Let us emphasize that the functional $s[\phi]$ is expressed in terms of the *free* boundary tiling entropy σ , whatever the conditions on the boundary $\partial\mathcal{D}$ of the domain \mathcal{D} . An example of smooth function ϕ is displayed in figure 2.

2.3. Dominant states in the statistical ensemble

The faceted membranes defined on \mathcal{D} that have the good boundary conditions are counted by

$$\mathcal{N} = \int_{\phi \in F} \mathcal{D}\phi \exp[Ns[\phi]]. \quad (15)$$

This functional integral is taken upon the set F of functions which are smooth representations of faceted membranes.

† More precisely, the coarse-graining is a convolution product of ϕ and another function of spatial extension a_0 .

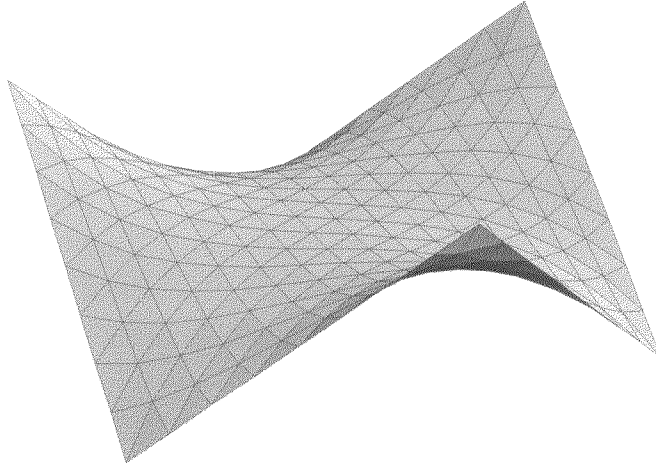


Figure 2. A smooth function $\phi : \mathbf{R}^2 \rightarrow \mathbf{R}$ and its frame, in the $3 \rightarrow 2$ case.

Moreover, the entropy per tile associated with this set of all the membranes (or tilings) is given by

$$S = \lim_{N \rightarrow \infty} \frac{\log \mathcal{N}}{N}. \quad (16)$$

Now, we suppose that there exists a unique function ϕ_{\max} that maximizes the entropy functional $s[\phi]$. This point will be discussed at the end of this section. Moreover, we suppose that the functional is non-singular near this maximum, i.e. it has a quadratic behaviour:

$$s[\phi] = s[\phi_{\max}] - \int_{\mathcal{D}} d^d u \int_{\mathcal{D}} d^v k_{u,v} (\phi(u) - \phi_{\max}(u), \phi(v) - \phi_{\max}(v)) + \dots \quad (17)$$

where k is a positive quadratic form, which *a priori* depends on the point (u, v) .

Hence, near ϕ_{\max} , \mathcal{N} is a Gaussian functional integral, and thanks to a generalized saddle-point argument, we obtain

$$\begin{aligned} S &= \lim_{N \rightarrow \infty} \frac{\log(\mathcal{N})}{N} \\ &= s[\phi_{\max}]. \end{aligned}$$

This is a classical result in statistical physics: at the infinite-size limit, the total entropy is equal to the entropy of a dominant macroscopic state. In other words, the statistical ensemble of faceted membranes is dominated by membranes close to ϕ_{\max} . In the space of membranes, the distribution is ‘peaked’ around ϕ_{\max} at the infinite-size limit, and looks more and more like a Dirac distribution.

To close this section, we must discuss the assumption of uniqueness of ϕ_{\max} . We shall use a general convexity argument: if a function f is strictly concave on a convex set C and if f has a maximum on C , then this maximum is unique.

Now, the set F of functions is convex: whatever their boundary conditions on $\partial\mathcal{D}$, let ϕ_1 and ϕ_2 be any two smooth functions in F and let λ be any real number between 0 and 1, then $\phi_\lambda = \lambda\phi_1 + (1 - \lambda)\phi_2$ is also an element of F . In particular, if $\nabla\phi_1$ and $\nabla\phi_2$ satisfy the good conditions to insure that ϕ_1 and ϕ_2 are in F , by linearity of the gradient, $\nabla(\lambda\phi_1 + (1 - \lambda)\phi_2)$ satisfies the same conditions; whatever the boundary conditions, ϕ_λ also satisfies them.

Let us now check whether $s[\phi]$ is concave: it is an integral, and therefore a positive linear combination of functions of ϕ (the entropies per unit area). If we prove that all these functions are concave, then it follows that $s[\phi]$ is concave. Now, the entropy at the point y in \mathcal{D} is the composition of $\tau(\mathbf{E})$ and the function $\phi \mapsto \nabla\phi(y)$, which is in turn a linear function. Hence we only need to prove that $\tau(\mathbf{E})$ is a concave function of \mathbf{E} .

This property is a little stronger than the general *random tiling model* hypothesis, which states that the free entropy has a unique maximum as a function of the gradient \mathbf{E} , and is quadratic near this maximum [4]:

$$\tau^{\text{free}}(\mathbf{E}) \simeq \tau_0^{\text{free}} - \frac{1}{2} K^{\text{free}} \mathbf{E}^2 \tag{18}$$

where K^{free} is the so-called tensor of phason elastic constants. Even if our stronger hypothesis is *a priori* valid for a more restricted set of models, let us note that it is satisfied in all exactly solvable tiling models [21–24]†. The concavity of $s[\phi]$ and the uniqueness of ϕ_{max} are therefore reasonable hypotheses.

Finally, let us remark that since this maximum is unique, it will respect all the underlying symmetries of the problem. We shall see an illustration of this fact in the following.

3. Relationship between different boundary conditions

In principle, whenever the free boundary entropy τ is known, the functional $s[\phi]$ is precisely defined, and one can therefore get the fixed boundary entropy. Theoretically, we are able to deduce the maximum entropy of fixed boundary tilings, τ_0^{fixed} , as well as the phason elastic constants, K^{fixed} , from their counterpart in the free boundary case, τ_0^{free} et K^{free} , and to invert these relations. This was done in the $3 \rightarrow 2$ case, in [10]‡, in the so-called quadratic approximation, which consists of estimating the free boundary entropy by its quadratic development (equation (18)) near its maximum. Here, we shall go further and give a complete treatment of this $3 \rightarrow 2$ case. We shall also present some related work in the case of different fixed boundary conditions.

To go beyond the quadratic approximation, we shall characterize the maximum of the entropy functional $s[\phi]$ by means of a functional derivation. If $s[\phi] = \int_{\mathcal{D}} n(\nabla\phi)\sigma(\nabla\phi) \, d^d y$, then

$$\begin{aligned} \delta s &= s[\phi + \delta\phi] - s[\phi] \\ &= \frac{1}{V(\mathcal{D})} \int_{\mathcal{D}} d\tau (\nabla\phi(y)) \cdot \nabla(\delta\phi) \, d^d y \\ &= \frac{-1}{V(\mathcal{D})} \int_{\mathcal{D}} \delta\phi \operatorname{div}(d\tau) \, d^d y. \end{aligned} \tag{19}$$

Hence,

$$\frac{\delta s}{\delta\phi(y)} = -\operatorname{div}(d\tau (\nabla\phi(y))). \tag{20}$$

Therefore ϕ_{max} is the function ϕ which satisfies this equation and which has good boundary conditions.

† A class of tilings is known to violate this hypothesis [25], but this is a quite singular case: the (unique) maximum coincides with a phase transition and is thus not of quadratic nature.

‡ In this reference, the value 0.253 of the diagonal entropy in the quadratic approximation was erroneous, because of badly controlled boundary effects. The actual value is 0.251.

3.1. Hexagonal tilings

Expression (20) is general. In the $3 \rightarrow 2$ case, it reads

$$\frac{\partial^2 \tau}{\partial E_1^2} \frac{\partial^2 \phi}{\partial x^2} + 2 \frac{\partial^2 \tau}{\partial E_1 \partial E_2} \frac{\partial^2 \phi}{\partial x \partial y} + \frac{\partial^2 \tau}{\partial E_2^2} \frac{\partial^2 \phi}{\partial y^2} = 0 \quad (21)$$

where $\mathbf{E} = (E_1, E_2)$.

The coefficients $\frac{\partial^2 \tau}{\partial E_1^2}$, $\frac{\partial^2 \tau}{\partial E_1 \partial E_2}$ and $\frac{\partial^2 \tau}{\partial E_2^2}$ are known. Indeed, in the $3 \rightarrow 2$ case, there exists an analogy between the tilings and the ground states of an antiferromagnetic Ising model on a triangular lattice [21]. The entropy can then be derived from the previous solution of this Ising model [26]. In the latter reference, the entropy is written in terms of chemical potentials. Some algebraic manipulations are therefore necessary to write it in terms of \mathbf{E} , and then obtain the above coefficients [11]:

$$\frac{\partial^2 \tau}{\partial E_1^2} = -\frac{\pi}{9} \frac{1}{\sin \theta} \left(\frac{1+w^2}{1-w^2} - \cos \theta \right) \quad (22)$$

$$\frac{\partial^2 \tau}{\partial E_1 \partial E_2} = \frac{\pi}{3\sqrt{3}} \frac{w}{\sin \theta} \frac{2-w^2}{1-w^2} \quad (23)$$

$$\frac{\partial^2 \tau}{\partial E_2^2} = -\frac{2\pi}{3} \frac{w}{1-w^2} \frac{1}{\sin \phi} \quad (24)$$

where $\theta = \frac{\pi\sqrt{2}}{3}(E_1 + \sqrt{2})$, $\phi = \sqrt{\frac{2}{3}}\pi E_2$, and $w = \tan(\theta/2)\cotan(\phi/2)$.

The partial differential equation (21) can be solved by means of numerical calculations. The idea is to discretize the domain \mathcal{Z} , which is a hexagon in this case, and to use an iterative process: at each step, a function ϕ_k is computed. The above coefficients are calculated in terms of ϕ_k . Then ϕ_{k+1} is the solution of a linear system which is the discrete version of equation (21). The sought function is the fixed point of this iterative process, which is reached after about 10 iterations. This method was used in [11] and gave satisfactory numerical results.

However, more recently, we were aware of related works by mathematicians who are interested in similar problems. They are indeed able to exactly compute the function ϕ_{\max} means of purely combinatoric methods [27, 28]: the idea is to calculate the number of fixed boundary tilings with a precise distribution of vertical tiles upon a given horizontal line. The value of ϕ_{\max} on this horizontal line is then given by the distribution of vertical tiles which maximizes the number of such tilings at the infinite-size limit.

This exact solution points up a very singular phenomenon. The above authors called it the *arctic circle phenomenon*: at the infinite-size limit, in the tiling representation in two dimensions, there is a central region of ε which is circular in the diagonal case and elliptic in general, inside which the tiling is random—in this sense that it contains the three kinds of tiles. Outside this region, the tiling is ‘frozen’: as illustrated in figure 3, there are six regions where there are only one kind of tiles, and where the entropy is equal to zero.

In these regions, the function ϕ_{\max} is rigorously linear and its gradient is constant. Inside the central region, in the diagonal case, the phason gradient of ϕ_{\max} is equal to [27]:

$$E_1 = -\sqrt{2} + \frac{3}{\pi\sqrt{2}} [\cotan^{-1} f(x, y) + \cotan^{-1} f(-x, y)] \quad (25)$$

$$E_2 = \frac{1}{\pi} \sqrt{\frac{3}{2}} [\cotan^{-1} f(x, y) - \cotan^{-1} f(-x, y)] \quad (26)$$

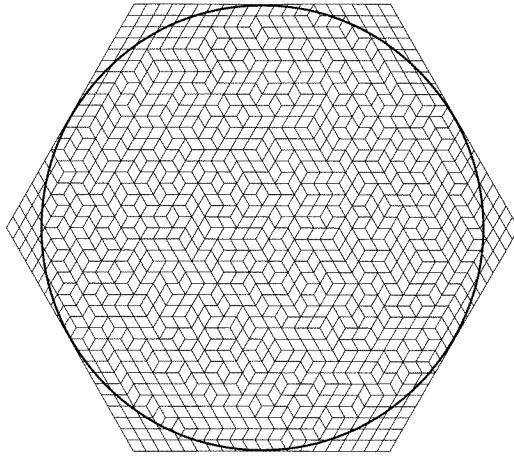


Figure 3. A randomly generated $3 \rightarrow 2$ tiling. At the infinite-size limit, there is a circular central region (the ‘arctic circle’ [25]), where the tiling contains three kinds of tiles, and six ‘triangular’ regions, where the tiling contains only one kind of tiles and is said to be ‘frozen’.

where $f(x, y) = \frac{1}{2\sqrt{3}} \frac{8/\sqrt{3}xy - \frac{8}{3}y^2 + 2}{\sqrt{1 - 4/3(x^2 + y^2)}}$, if the side of the hexagon has been rescaled to 1. In this expression and the previous ones, the origin of the coordinates is at the centre of the hexagon, the axis (Ox) is pointed towards a vertex of the hexagon.

These expressions characterize ϕ_{\max} . In fact, the resulting function is very close to the function showed in figure 2, which was actually computed in the quadratic approximation (17) [10]. Now, it is possible to compute the entropy per tile associated with ϕ_{\max} : a simple numerical calculation gives $S[\phi_{\max}] = 0.2616(3)$. This value is in exact agreement with the exactly known diagonal entropy of fixed boundary tilings. These results are therefore a validation of our continuous approach (coarse graining). As announced, we have established an exact link between free and fixed boundary tilings.

This function ϕ_{\max} deserves a quick qualitative description; since ϕ_{\max} is very close to the function displayed in figure 2, we shall use this figure to illustrate our arguments: first, when the boundary is an hexagon, it has a threefold symmetry and, as foreseen, the solution ϕ_{\max} respects this symmetry. Second, because of the strong influence of the boundary, there is a gradient of entropy between the boundary and the bulk. Indeed, near the centre of the tiling, the gradient of ϕ_{\max} is very close to the free boundary one, whereas far from the centre, this gradient becomes more and more influenced by the boundary and becomes singular out of the arctic circle; there, the entropy is zero. The fixed boundary tilings provide a very interesting model having an inhomogeneous entropy distribution.

To close this discussion, let us emphasize that this infinite-size limit cannot be called a ‘thermodynamic limit’ because of this lack of homogeneity: in statistical mechanics, a system is said to be at the thermodynamic limit if its properties do not depend on how it tends to infinity. In particular, they must be homogeneous in the system and must not depend on the container shape (here, the boundary) [20]. Here, the situation is far from this one, since even the stoichiometry depends on the boundary shape.

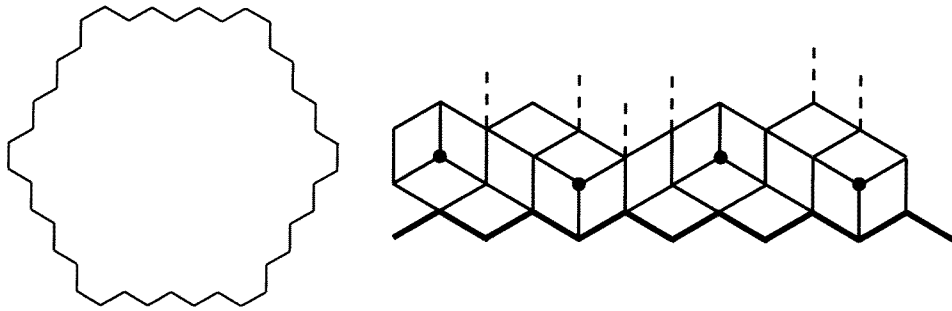


Figure 4. Left: a zigzag boundary, without phason strain. Right: tiling detail; the boundary (heavy line) is globally—but not locally—straight.

3.2. Other kinds of tilings

So far, we have only considered zonotopal fixed boundaries. The reason for this choice is that the first motivation of this work was to establish the link between free boundary tilings and tilings built by means of the so-called partition method, the aim of which was to develop a new approach to these tiling questions [7–11]. The latter tilings precisely have zonotopal boundary conditions, by construction. However, there is no reason why the previous method could not be applied to other kinds of boundaries. In this section, we shall analyse tilings, the boundary of which is fixed, but which nevertheless have a free boundary entropy.

Indeed, if the boundary is fixed but imposes a uniform phason gradient, that is to say the membrane frame lies in a d -dimensional plane of gradient $\mathbf{E} = \mathbf{E}_0$, then the affine membrane of gradient \mathbf{E}_0 has on the one hand good boundary conditions, and on the other hand satisfies the partial differential equation (21) (since its second-order derivatives are equal to zero). This membrane is therefore the function ϕ_{\max} and its entropy $s[\phi_{\max}]$ is equal to the free boundary one, $\tau(\mathbf{E}_0)$.

More precisely, let us analyse a $3 \rightarrow 2$ class of tilings, the fixed boundary of which is *flat* in the membrane representation in three dimensions, that is to say does not impose any global phason strain to the tilings. This kind of boundary is illustrated in figure 4.

At the infinite-size limit and in the membrane point of view, after rescaling, the boundary becomes a flat hexagon: the function ϕ is constrained to zero on this boundary. Therefore the function $\phi = 0$ maximizes the entropy and, at the infinite-size limit, this entropy is equal to σ_0^{free} .

We have tested this theoretical prediction by a direct calculation of this entropy. The method is developed in appendix A.3. It uses again the Gessel–Viennot method [18, 19]. The entropy of very large tilings can then be numerically reached and fitted to get its infinite-size limit. We find an entropy per tile of 0.323 06(4), which is precisely the free boundary entropy.

To close this section, let us draw attention to numerical simulations by Joseph and Baake [29]: they analysed the configurational entropy of random $4 \rightarrow 2$ tilings, the boundary of which is fixed and flat (in four dimensions), as in our previous example (the global phason strain is zero). As foreseen, the entropy that they eventually found was equal to the free boundary one, which was itself numerically estimated.

4. Conclusion

Thanks to a continuous approach in the membrane point of view at the infinite-size limit, we have been able to describe the dominant states of statistical ensembles of tilings. In particular, this method has enabled us to establish a quantitative link between two exactly solvable models of statistical mechanics, the free and fixed boundary tilings of 60 degree rhombi. In the latter, a very remarkable event occurs, the arctic circle phenomenon: there exist ‘frozen’ regions of the tilings in which there is only one kind of tile and where the entropy is therefore zero. This lack of homogeneity is responsible for the difference of entropy between the two problems, even if they are at first sight closely related. Moreover, this infinite-size limit cannot be called a thermodynamic limit because of this lack of homogeneity.

In the case of larger dimension or codimension tilings, a similar treatment would require the knowledge of the free boundary entropies. Unfortunately, despite a great deal of work, these entropies are not known yet. However, the maximum (diagonal) entropies and the phason elastic constants are numerically known in many cases. It could therefore be possible, in these cases, to compute the fixed boundary entropies and phason elastic constants, in the quadratic approximation. However, this approximate method would not be conclusive on the existence of an arctic circle phenomenon in such problems, which is nevertheless a captivating open question.

Finally, it is worth emphasizing that this method could be useful in describing how any constraint imposed at the boundary relaxes into the bulk. In this paper, we have studied two kinds of boundaries. The first one, the straight boundary related to partition problems, imposes to the tiling the strongest constraint among all boundary conditions: the tilings must relax continuously from a completely crystalline structure to a random one. Physically, such tilings (in three dimensions) could model the result of a growth of quasicrystalline materials on crystalline phases. More generally, more complex physical situations, such as extended topological defects (such as dislocations), or other kinds of interfaces, could *a priori* be translated in suitable boundary conditions. The numerical method we have developed could then be applied to any such boundary conditions and could be useful in describing how the material relaxes in the presence of such constraints.

Note added in proof. We have recently been made aware of related works in the Aztec diamond tiling problem [30].

Appendix. The Gessel–Viennot method

In this appendix, we present a combinatorial method for the counting of configurations of avoiding paths on planar graphs, the Gessel–Viennot method, which can be very useful in the enumeration of fixed boundary tilings. We illustrate this method in two $3 \rightarrow 2$ cases discussed in this paper.

A.1. The method

We shall not extensively present the Gessel–Viennot method [18, 19]. We shall instead give a brief description and try to explain the underlying ideas. The method is rather general: it can be applied to any oriented graph without cycles (acyclic oriented graph), in which two families of vertices, u_i and v_i , $i = 1, \dots, n$, are selected. This graph is supposed to satisfy

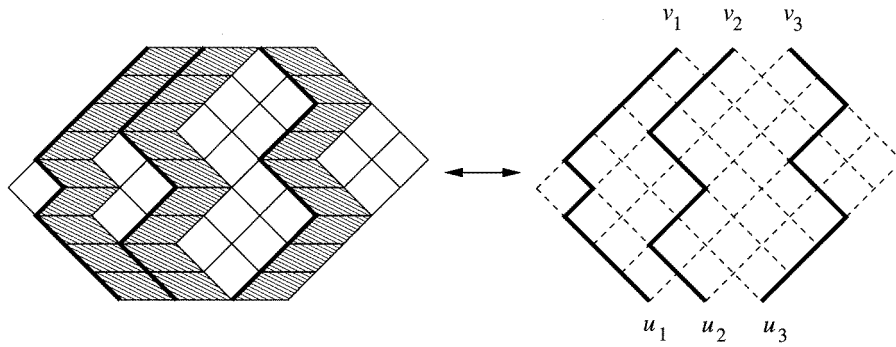


Figure 5. A hexagonal boundary $3 \rightarrow 2$ tiling (left): the broken worms can be translated into a set of p avoiding oriented paths on a square lattice (right). The i th path starts from the (fixed) vertex u_i and goes to the (fixed) vertex v_i . There are p paths. The side lengths of the hexagon are p , k and l .

the property of *compatibility*: if two paths on this graph are going respectively from u_{i_1} to v_{j_1} and from u_{i_2} to v_{j_2} and if these paths do not cross, then $i_1 < i_2$ and $j_1 > j_2$. Note that this property is very specific to two-dimensional graphs.

We are interested in the number of configurations of n avoiding (or non-intersecting) paths, the i th path going from u_i to v_i . If we denote by λ_{ij} the number of paths going from u_i to v_j , then the method states that the number of configurations is equal to the following determinant:

$$D_n = \det(\lambda_{ij})_{1 \leq i, j \leq n}. \quad (27)$$

The idea of the proof is the following: in this determinant, all path configurations, whether intersecting or not, the i th path going from u_i to $v_{\sigma(i)}$, for any permutation σ , are counted, with a $+$ or $-$ sign. All interesting configurations cancel two by two and only the non-intersecting configurations remain. They are exactly the sought configurations thanks to the property of compatibility. The reader interested in more details can refer to the review paper by Stembridge [19].

A.2. Hexagonal boundaries

In this section, the previous method will be used to rederive MacMahon's formula (see section 1). Consider a $3 \rightarrow 2$ tiling of a hexagonal region of side lengths k , l and p (figure 5, left). In such a tiling, one can follow sequences of tiles which have a horizontal edge. These lines, which are usually called worms, cross the tiling from bottom to top. The tiling can now be slightly deformed so that a kind of tiles become squares (figure 5) and the p worms can be seen as up-going paths on a square lattice (figure 5, right).

Therefore the previous theory on avoiding paths on an acyclic oriented graph can be applied. The number λ_{ij} of paths joining the vertices u_i and v_j is a binomial coefficient:

$$\lambda_{ij} = \frac{(k+l)!}{(k+j-i)!(l+i-j)!}. \quad (28)$$

We have to compute the following determinant:

$$D_p(k, l) = \det(\lambda_{ij}) = \det \left[\frac{(k+l)!}{(k+j-i)!(l+i-j)!} \right]_{1 \leq i, j \leq p} \quad (29)$$

$$\begin{aligned}
 D_p(k, l) &= [(k + l)!]^p \det \left[\frac{1}{(k + j - i)!(l + i - j)!} \right]_{1 \leq i, j \leq p} \\
 &= [(k + l)!]^p \frac{1}{(k + p - 1)! \dots k!} \frac{1}{(l + p - 1)! \dots l!} \\
 &\quad \times \det \left[\frac{(k + p - i)!(l + i - 1)!}{(k + j - i)!(l + i - j)!} \right]_{1 \leq i, j \leq p}. \tag{30}
 \end{aligned}$$

The first factor equals $[(k + l)!]^p \frac{(k-1)!^{[2]} (l-1)!^{[2]}}{(k+p-1)!^{[2]} (l+p-1)!^{[2]}}$, where we have used again the second-order factorial function. The second factor is denoted by Δ_p . We shall use the notation: $P_j^{(p)}(i) = \frac{(k+p-i)!(l+i-1)!}{(k+j-i)!(l+i-j)!}$. Since $j \leq p$, $P_j^{(p)}$ is a polynomial of degree $(p - j) + (j - 1) = p - 1$.

We now use the following result concerning polynomials: if $Q_j, j = 1, \dots, p$ are polynomials of degree smaller than $p - 1$, if $Q_j = \sum_{i=0}^{p-1} a_i^{(j)} X^i$, and if x_1, x_2, \dots, x_p are real numbers, then

$$\det[Q_j(x_i)]_{1 \leq i, j \leq p} = \det(a_i^{(j)}) \times \text{VdM}(x_1, \dots, x_p) \tag{31}$$

where $\text{VdM}(x_1, \dots, x_p)$ is the Van der Monde determinant of these real numbers. We recall that

$$\text{VdM}(x_1, \dots, x_p) = \begin{vmatrix} 1 & x_1 & x_1^2 & \dots & x_1^{p-1} \\ 1 & x_2 & x_2^2 & \dots & x_2^{p-1} \\ \vdots & \vdots & \vdots & & \vdots \\ 1 & x_p & x_p^2 & \dots & x_p^{p-1} \end{vmatrix}. \tag{32}$$

The proof of equation (31) is straightforward: the left-hand side matrix is the product of the coefficient matrix and of the Van der Monde matrix. Note that $\text{VdM}(1, 2, \dots, p) = (p - 1)!^{[2]}$.

Now, the calculation of Δ_p is made by induction on p : if d_p denotes the determinant of the coefficients of the polynomials $P_j^{(p)}, j = 1, \dots, p$, then thanks to the above results, $\Delta_{p+1} = p!^{[2]} d_{p+1}$. After a tedious calculation, one finds that

$$\frac{d_{p+1}}{d_p} = P_{p+1}^{(p+1)}(k + p + 1) = (k + l + p) \dots (k + l + 1). \tag{33}$$

So by induction on p ,

$$d_p = \frac{1}{[(k + l)!]^p} \frac{(k + l + p - 1)!^{[2]}}{(k + l - 1)!^{[2]}}. \tag{34}$$

Finally, we obtain

$$D_p(k, l) = \frac{(k + l + p - 1)!^{[2]}(k - 1)!^{[2]}(l - 1)!^{[2]}(p - 1)!^{[2]}}{(k + p - 1)!^{[2]}(l + p - 1)!^{[2]}(k + l - 1)!^{[2]}} \tag{35}$$

which is precisely MacMahon’s enumerative formula (17), rewritten in terms of generalized factorials.

A.3. Flat fixed boundaries

This method can also be applied to the tilings studied in section 3.2 (figure 4). However, in this case, we shall not be able to get an explicit enumerative formula and some numerical calculations will be necessary to have access to the infinite-size entropy.

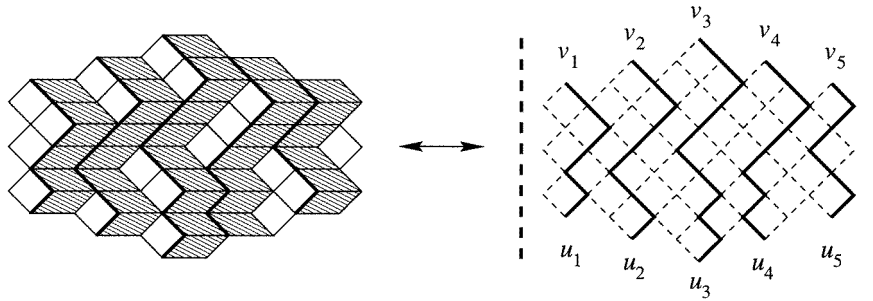


Figure 6. The worm representation of a flat-boundary tiling (left) and its counterpart in the avoiding path representation (right), in the case when the number of lines n is equal to 5.

Table A1. Entropy per tile of n -worm tilings with flat boundaries. These boundaries do not impose any global phason strain.

Number of worms	Entropy per tile
$n = 21$	$S = 0.311\,881$
$n = 31$	$S = 0.315\,379$
$n = 61$	$S = 0.319\,098$
$n = 81$	$S = 0.320\,065$
$n = 101$	$S = 0.320\,653$
$n = 151$	$S = 0.321\,446$

With these boundary conditions, the worm and path representations of figure 5 must be modified, as illustrated in figure 6.

The two main differences are the following: first, the vertices u_i and v_i are not as simply distributed as in figure 5. Second, some of the n paths are constrained by the presence of two vertical bounds (heavy broken curves). Therefore, the number λ_{ij} of paths starting from u_i and going to u_j might be different from a simple binomial coefficient. This number can be calculated thanks to the usual ‘mirror’ or ‘image method’ (see [31], for instance). In the diagonal case, with the indexation of figure 6 and when n is odd,

$$\lambda_{ij} = \binom{p_{ij}}{\frac{p_{ij}+3(i-j)}{2}} - \binom{p_{ij}}{\frac{p_{ij}+3(i+j)-2}{2}} - \binom{p_{ij}}{\frac{p_{ij}+6n-3(i+j)+4}{2}} \quad (36)$$

where

$$p_{ij} = 2n = \left| \frac{n+1}{2} - j \right| - \left| \frac{n+1}{2} - i \right| \quad (37)$$

is the length of any path going from u_i to v_j .

The method is now strictly similar to the previous one. However, the complete calculation of the determinant $\det(\lambda_{ij})$ seems out of reach. That is why we have chosen to compute it numerically for large systems. The so-obtained values are displayed in table A1. In this table, n still denotes the number of worms.

The last four data can be fitted with the following law:

$$S(n) = S_0 - \frac{A}{n} + \frac{B}{n^2} \quad (38)$$

we get $S_0 = 0.323\,06(4)$, which is the infinite-size entropy (and $A \simeq 0.246$, $B \simeq 0.245$).

References

- [1] Shechtman D, Blech I, Gratias D and Cahn J W 1984 Metallic phase with long-range orientational order and no translational symmetry *Phys. Rev. Lett.* **53** 1951
- [2] Penrose R 1974 The role of aesthetics in pure and applied mathematical research *Bull. Inst. Math. Appl.* **10** 226
- [3] Elser V 1985 Comment on quasicrystals: a new class of ordered structures *Phys. Rev. Lett.* **54** 1730
- [4] Henley C L 1991 Random tiling models *Quasicrystals, the State of the Art* ed D P Di Vincenzo and P J Steinhardt (Singapore: World Scientific) p 429
- [5] Widom M, Deng D P and Henley C L 1989 Transfer-matrix analysis of a two-dimensional quasicrystal *Phys. Rev. Lett.* **63** 310
- [6] Strandburg K J, Tang L H and Jarić M V 1989 Phason elasticity in entropic quasicrystals *Phys. Rev. Lett.* **63** 314
- [7] Elser V 1984 Solution of the dimer problem on an hexagonal lattice with boundary *J. Phys. A: Math. Gen.* **17** 1509
- [8] Mosseri R, Bailly F and Sire C 1993 Configurational entropy in random tiling models *J. Non-Cryst. Solids* **153–154** 201
- [9] Mosseri R and Bailly F 1993 Configurational entropy in octagonal tiling models *Int. J. Mod. Phys. B* **6–7** 1427
- [10] Destainville N, Mosseri R and Bailly F 1997 Configurational entropy of codimension-one tilings and directed membranes *J. Stat. Phys.* **87** 697
- [11] Destainville N 1997 *PhD Thesis* Entropie configurationnelle des pavages aléatoires et des membranes dirigées *Thèse de l'Université Paris 6*
- [12] Wannier G H 1950 Anti-ferromagnetism. The triangular Ising net *Phys. Rev.* **79** 357
Wannier G H 1973 *Phys. Rev. B* **7** 5017
- [13] Destainville N, Mosseri R and Bailly F 1997 Role of boundary conditions in configurational entropy of random tilings *Proc. 6th Int. Conf. on Quasicrystals* (Singapore: World Scientific)
- [14] Duneau M and Katz A 1985 Quasiperiodic patterns *Phys. Rev. Lett.* **54** 2688
- [15] Kalugin A P, Kitaev A Y and Levitov L S 1985 $\text{Al}_{0.86}\text{Mn}_{0.14}$: a six-dimensional crystal *JETP Lett.* **41** 145
Kalugin A P, Kitaev A Y and Levitov L S 1985 6-dimensional properties of $\text{Al}_{0.86}\text{Mn}_{0.14}$ *J. Physique Lett.* **46** L601
- [16] Coxeter H S M (ed) 1973 *Regular Polytopes* (New York: Dover)
- [17] MacMahon P A (ed) 1916 *Combinatory Analysis* (Cambridge: Cambridge University Press)
- [18] Gessel I and Viennot G 1985 Binomial determinants, paths, and hook length formulae *Adv. Math.* **58** 300–21
- [19] Stembridge J M 1990 Non-intersecting paths, pfaffians, and plane partitions *Adv. Math.* **83** 96–131
- [20] Toda M, Kubo R and Saitō N (ed) 1982 *Statistical Physics* vol I (Berlin: Springer)
- [21] Blöte H W J and Hilhorst H J 1982 Roughening transitions and zero-temperature triangular Ising anti-ferromagnet *J. Phys. A: Math. Gen.* **15** L631
- [22] Kalugin P A 1994 The square-triangle random-tiling model in the thermodynamic limit *J. Phys. A: Math. Gen.* **27** 3599
- [23] de Gier J and Nienhuis B 1996 Exact solution of an octagonal random tiling model *Phys. Rev. Lett.* **76** 2918
- [24] de Gier J and Nienhuis B 1998 Bethe ansatz solution of a decagonal rectangle-triangle random tiling *J. Phys. A: Math. Gen.* **31** 2141
- [25] Richard C, Höffe M, Hermisson J and Baake M 1998 Random tilings: concepts and examples *J. Phys. A: Math. Gen.* **31** 6385
- [26] Houtappel R M F 1950 *Physica* **16** 425
- [27] Cohn H, Larsen M and Propp J The shape of a typical boxed plane partition *NY J. Math.* submitted
- [28] Propp J 1997 Boundary-dependent local behavior for 2-D dimer models *Int. J. Mod. Phys. B* **11** 183
- [29] Joseph D and Baake M 1996 Boundary conditions, entropy, and the signature of random tilings *J. Phys. A: Math. Gen.* **29** 6709
- [30] Cohn H, Kenyon R and Propp J A variational principle for domino tilings *Preprint*
- [31] Montroll E W and West B C J 1987 On an enriched collection of stochastic processes *Fluctuation Phenomena* ed E W Montroll and J L Lebowitz (Amsterdam: North-Holland)